

# Thermoelectric microstructures of $\text{Bi}_2\text{Te}_3/\text{Sb}_2\text{Te}_3$ for a self-calibrated micro-pyrometer

L.M. Goncalves<sup>a,\*</sup>, C. Couto<sup>a</sup>, P. Alpuim<sup>b</sup>, D.M. Rowe<sup>c</sup>, J.H. Correia<sup>a</sup>

<sup>a</sup> University of Minho, Department of Industrial Electronics, Campus de Azurem, 4800-058 Guimaraes, Portugal

<sup>b</sup> University of Minho, Department of Physics, Campus de Azurem, 4800-058 Guimaraes, Portugal

<sup>c</sup> University of Cardiff, School of Engineering, The Parade, Cardiff CF24 3AA, Wales, UK

Received 3 June 2005; received in revised form 28 September 2005; accepted 12 October 2005

Available online 21 November 2005

## Abstract

The fabrication of thermopiles suitable for thermoelectric cooling and energy generation using  $\text{Bi}_2\text{Te}_3$  and  $\text{Sb}_2\text{Te}_3$  as n- and p-type layers, respectively, is reported. The thin-film thermoelectric material deposition process, thin-film electronic characterization and device simulation is addressed.

The thermoelectric thin-films were deposited by co-evaporation of Bi and Te, for the n-type element and Sb and Te, for the p-type element. Seebeck coefficients of  $-190$  and  $+150 \mu\text{V K}^{-1}$  and electrical resistivities of  $8$  and  $15 \mu\Omega \text{m}$  were measured at room temperature on  $\text{Bi}_2\text{Te}_3$  and  $\text{Sb}_2\text{Te}_3$  films, respectively. These values are better than those reported in the literature for films deposited by co-sputtering or electrochemical deposition and are close to those reported for films deposited by metal-organic chemical vapour deposition and flash evaporation.

A small device with a cold area of  $4 \text{ mm} \times 4 \text{ mm}^2$  and four pairs of p–n junctions was fabricated on a Kapton<sup>®</sup> substrate, showing the possibility of application in Peltier cooling, infrared detection and energy generation.

Small devices fabricated on a polyimide (Kapton<sup>®</sup>) substrate and micro-devices fabricated on a silicon nitride substrate were simulated using finite element analysis. The simulations show the possibility of achieving near  $20 \text{ K}$  cooling over  $1 \text{ mm}^2$  areas.

© 2005 Elsevier B.V. All rights reserved.

**Keywords:** Thermoelectric; Thin-film; Pyrometer; Peltier; Micro-cooler;  $\text{Bi}_2\text{Te}_3$

## 1. Introduction

Thermoelectric cooling is widely employed in electronics to stabilize the temperature of devices, decrease noise levels and increase operation speed. And since Peltier devices are reversible, they can also be used as electrical generators, converting thermal into electrical energy. Commercial Peltier devices are usually fabricated on a transversal (cross-plane) configuration (Fig. 1). In theory, this configuration could be reduced for micro-device fabrication, but the conventional fabrication processes are not scalable to the micrometer range. Using a lateral (in-plane) configuration (Fig. 2), thin-film techniques can be used to scale down the thermoelectric coolers and generators to micro-device dimensions [1]. In the present work, planar thin-film technology will be used to fabricate such devices.

The thermoelectric performance of the thermoelectric materials is characterized by the dimensionless figure of merit parameter ( $ZT$ ):

$$ZT = \frac{\alpha^2}{\rho\lambda} T \quad (1)$$

Where  $\alpha$  is the Seebeck coefficient,  $\rho$  the electrical resistivity,  $\lambda$  the thermal conductivity and  $T$  the temperature [2]. While the search for thermoelectric materials with higher figures of merit is going on [3] (with higher Seebeck coefficients, lower electrical resistivities and lower thermal conductivities), efforts are currently made to achieve compatibility with state-of-the-art electronic materials and in particular with silicon-wafer technology [4]. In this paper, the possibility of integration with next-generation flexible electronic devices is also demonstrated.

Tellurium alloys ( $\text{Bi}_2\text{Te}_3$  and  $\text{Sb}_2\text{Te}_3$ ) are well-established low-temperature thermoelectric materials and are widely employed in conventional thermoelectric generators and

\* Corresponding author. Tel.: +351 253510190; fax: +351 253510189.

E-mail address: [lgoncalves@dei.uminho.pt](mailto:lgoncalves@dei.uminho.pt) (L.M. Goncalves).

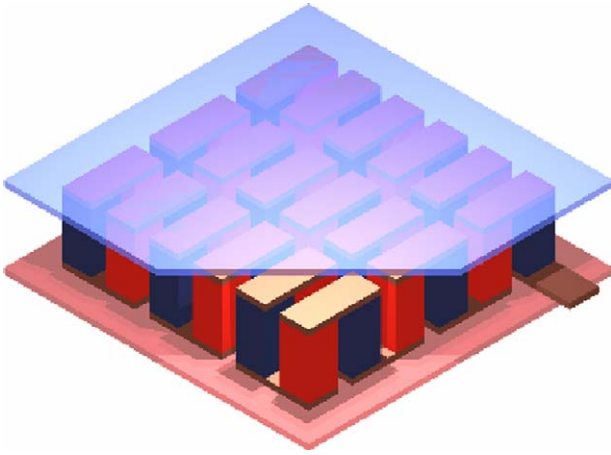


Fig. 1. Cross-plane (transversal) Peltier cooler.

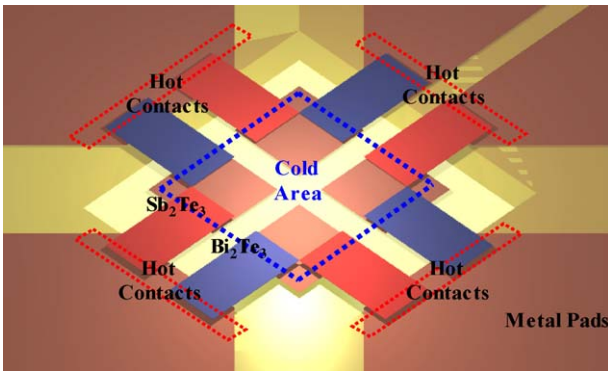


Fig. 2. In-plane (lateral) Peltier cooler.

coolers [2]. Different deposition techniques can be used to obtain Bi–Sb–Te thin-films. Thermal co-evaporation [5], co-sputtering [6], electrochemical deposition [7], metal-organic chemical vapour deposition [8] and flash evaporation [9] are some examples. In this work, thermoelectric energy converters are addressed, from simulation and performance prediction, to materials deposition and optimization and device fabrication. A Peltier cooler and a thermopile in a single device to implement a self-calibrated micro-pyrometer, operating in the 20–100 °C measuring range, is the final goal of this work.

## 2. Simulation

Each p–n thermoelectric pair of the Peltier cooler can be modelled [1] by Eq. (2).

$$\Delta T = \frac{1}{K_{eq}} \left[ (\alpha_p - \alpha_n) T_c I - \frac{1}{2} R_{eq} I^2 - Q_{LOAD} \right] \quad (2)$$

$\Delta T$  is the maximum temperature difference achieved by the cooler,  $\alpha_n$  and  $\alpha_p$  are the Seebeck coefficients of the n- and p-type materials,  $T_c$  is the cold side temperature,  $I$  is the current injected in the device and  $Q_{LOAD}$  is the sum of all thermal loads applied.  $R_{eq}$  and  $K_{eq}$  are the equivalent electrical resistance and thermal conductance of n- and p-type elements, including the effect of substrate and contact resistances, calculated with Eqs.

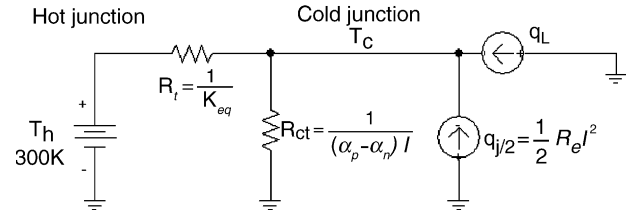


Fig. 3. Schematic model of a Peltier cooler.

(3) and (4):

$$R_{eq} = \rho_n \frac{L_n}{W_n H_n} + \rho_p \frac{L_p}{W_p H_p} + 2 \left( \frac{\rho_{cn}}{L_c W_n} + \frac{\rho_{cp}}{L_c W_p} \right) \quad (3)$$

$$K_{eq} = \lambda_n \frac{W_n H_n}{L_n} + \lambda_p \frac{W_p H_p}{L_p} + \lambda_m \frac{W_m H_m}{L_m} \quad (4)$$

where  $W$  is the width,  $H$  is the height,  $L$  is the length, the indexes n, p, m and c stand for n-type leg, p-type leg, membrane and contact, respectively,  $\rho$  is the electrical resistivity and  $\lambda$  is the thermal conductivity. Eq. (2) assumes that the hot side of the cooler is connected to a highly thermally conductive material and to a heat sink, capable of keeping the hot side of the device at room temperature. This can be achieved in a micro Peltier cooler for example by the use of a silicon substrate as the heat sink. For convenience of the simulation, Eq. (2) was implemented by the schematic shown in Fig. 3 using electrical simulation software.

For more complex structures, the use of more powerful finite element analysis tools is required. Two device types were simulated using finite element analysis:

- A small device (Figs. 2 and 9), with a cold area of 4 mm × 4 mm. This mini-device rests on a 25 μm-thick Kapton® membrane and has 4 p–n pairs of thermoelectric legs, each with dimensions of 2 mm × 1 mm × 10 μm.
- A micro-device (Figs. 4 and 10), with cold area smaller than 1 mm<sup>2</sup>, supported by a 1 μm-thickness silicon nitride air-gap bridge, cooled by three pairs of thermoelectric legs, with dimensions of 100 μm × 200 μm × 4 μm each. This device will be used to cool down a radiation sensor and a thermopile in a self-calibrated micro-pyrometer, as described below.

Results of the simulations show the possibility to obtain 18 K temperature difference with the mini-device and 10 K with the micro-device, after considering conduction, radiation and convection losses. Fig. 4 shows the temperature map simulated for a micro-cooler device.

The performance of the Peltier cooler is largely affected by the thickness and thermal conductivity of the supporting membrane used as substrate. This is shown in Fig. 5 where the temperature achieved with a thermoelectric cooler was simulated using Eqs. (2)–(4) and plotted as a function of the current injected in the device, for different material composition and thickness of the substrate membrane.

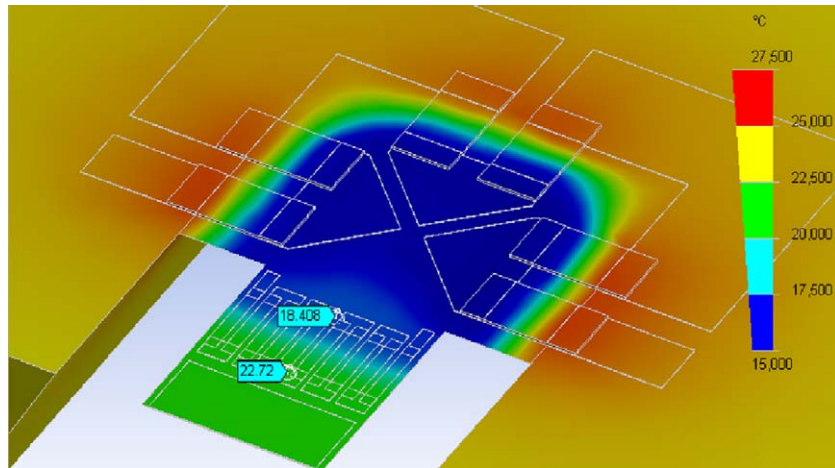


Fig. 4. Finite element analysis shows the possibility to obtain 10 K cooling in a micro-device.

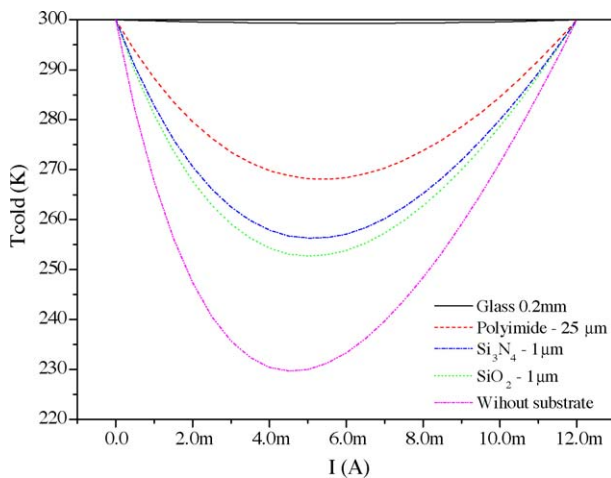


Fig. 5. The supporting membrane affects largely the performance of a lateral thermoelectric cooler.

### 3. Thin-film deposition

Bismuth, tellurium and antimony have large differences in vapour pressure. This difference resulted in a compositional gradient along the film thickness, when  $\text{Bi}_2\text{Te}_3$  and  $\text{Sb}_2\text{Te}_3$  films were directly evaporated from the compounds. This composition gradient effect is also reported in literature [10]. The problem of composition gradient can be overcome, though, by the use of co-evaporation [5]. Bi and Te were evaporated from two independently controlled molybdenum boats, in order to achieve  $\text{Bi}_2\text{Te}_3$  films. A similar procedure was adopted for  $\text{Sb}_2\text{Te}_3$  deposition from two independent Sb and Te sources. 15 mm  $\times$  15 mm, 25  $\mu\text{m}$ -thick flexible Kapton<sup>®</sup> foils were mounted on a resistive heater placed in the vacuum deposition chamber and used as substrates for all films and devices fabricated. Plastic film was chosen as substrate for being flexible, robust and having low-thermal conductivity. While plastic mechanical properties are advantageous for integration with any type of flexible electronic device, the specific choice of Kapton<sup>®</sup> was due to its high upper working temperature ( $>300^\circ\text{C}$ ), low-thermal conductivity ( $0.12 \text{ W m}^{-1} \text{ K}^{-1}$ ) and to its value of thermal expansion

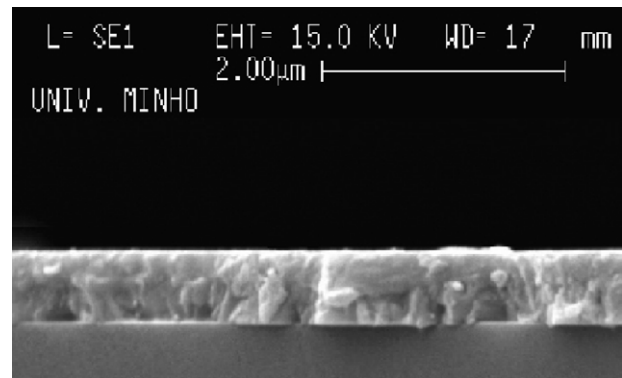


Fig. 6. A SEM photo of a homogeneous n-type 700 nm-thick  $\text{Bi}_2\text{Te}_3$  film.

coefficient ( $12 \times 10^{-6} \text{ K}^{-1}$ ) which closely matches the thermal expansion coefficient of the films, thus reducing residual stress and improving adhesion. The co-evaporation method is inexpensive, simple and reliable, when compared to other techniques that need longer time periods to prepare the starting material or require more complicated and expensive deposition equipment. During deposition the substrate was heated to temperatures in the range  $200\text{--}300^\circ\text{C}$ . Two crystal oscillators and thickness monitors were used to monitor the deposition rate of Bi/Sb and Te. Each rate was maintained at a fixed value, through independent control of the power applied to each molybdenum evaporation boat. A mini-device was also made by this technique, using aluminium as the contact material, covered with a thin layer of nickel, to decrease contact resistance between the thermoelectric material and the contact metal. Stainless steel masks were used to define the different n- and p-type layers and the contact pads. Fig. 6 shows a cross-section of a  $\text{Bi}_2\text{Te}_3$  film.

### 4. Results and measurements

Table 1 shows the composition, obtained by energy-dispersive X-ray spectroscopy (EDX), of the best n- and p-type films. Te and Bi (Sb) content shows that the composition of both types of films is close to stoichiometry. X-ray diffraction (XRD) analysis reveals the polycrystalline structure of the films. The



Table 1  
Measured properties of thermoelectric films

Film	Te (%)	Bi or Sb (%)	Seebeck ( $\mu\text{V}/^\circ\text{C}$ )	Hall mobility ( $\text{cm}^{-2} \text{V}^{-1} \text{s}^{-1}$ )	Resistivity ( $\mu\Omega \text{m}$ )	Figure of merit
$\text{Bi}_2\text{Te}_3$	60.17	39.83	-189	75	7.7	0.93
$\text{Sb}_2\text{Te}_3$	58.51	41.49	140	70	15.1	0.26

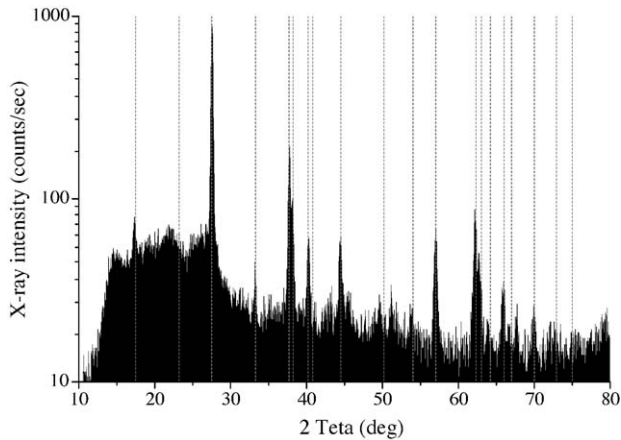


Fig. 7. A XRD analysis of an n-type  $\text{Bi}_2\text{Te}_3$  thin-film. The peaks agree with the powder diffraction spectrum for  $\text{Bi}_2\text{Te}_3$  (dashed lines).

peaks agree with the powder diffraction spectra for polycrystalline  $\text{Bi}_2\text{Te}_3$  (Fig. 7) and  $\text{Sb}_2\text{Te}_3$  (Fig. 8).

In-plane film electrical resistivity and hall mobility were measured using conventional four probe van der Pauw geometry, at room temperature. Seebeck coefficient was measured by connecting one side of the film to a heated metal block at a fixed temperature and the other side to a heat sink at room temperature. Table 1 also shows the results of these measurements and the corresponding figure of merit at 300 K (thermal conductivity of  $1.5 \text{ W m}^{-1} \text{ K}^{-1}$  was assumed for calculations).

Electronic properties and figures of merit of  $\text{Bi}_2\text{Te}_3$  films prepared in this work are as good as the best found in literature for the bulk material.  $\text{Sb}_2\text{Te}_3$  films could not attain the same high-level of performance although showing relatively high performance parameters.

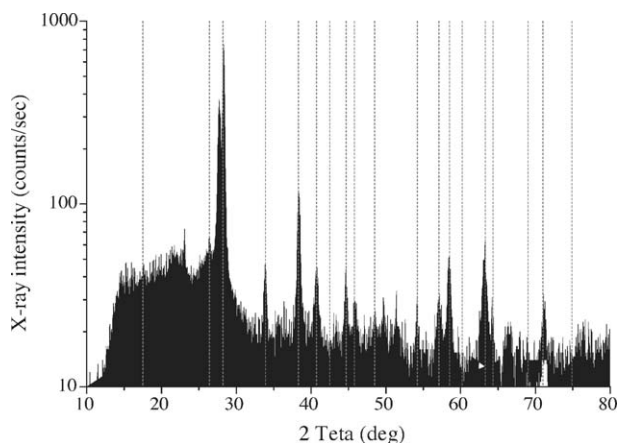


Fig. 8. A XRD analysis of an p-type  $\text{Sb}_2\text{Te}_3$  thin-film. The peaks agree with the powder diffraction spectrum for  $\text{Sb}_2\text{Te}_3$  (dashed lines).

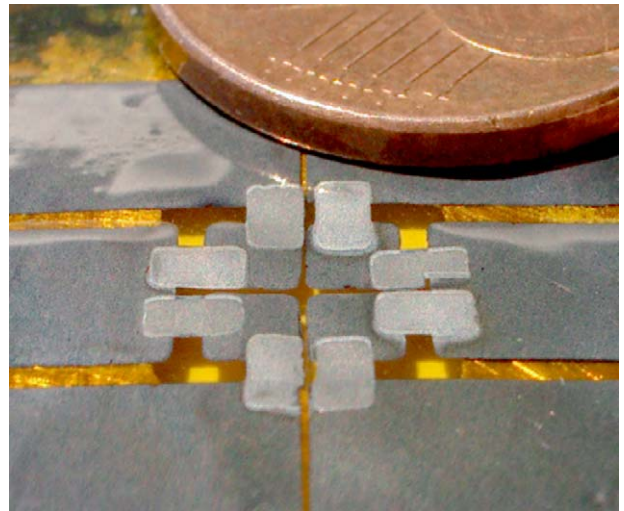


Fig. 9. Thermoelectric mini-device fabricated on kapton substrate.

Fig. 9 shows a mini-device fabricated on Kapton<sup>®</sup> device, with four pairs of Peltier junctions. Each thermoelectric leg has the thickness of  $2.3 \mu\text{m}$  and the metal contacts have thickness of  $0.5 \mu\text{m}$ . Seebeck coefficients of  $-169$  and  $+151 \mu\text{V K}^{-1}$  and electrical resistivities of  $12$  and  $17 \mu\Omega \text{m}$  were measured at room temperature in n- and p-type films, respectively, which represents a sensitivity in the thermopile higher than  $1.2 \text{ mV K}^{-1}$ . Due to technical problems during fabrication, the thickness of the fabricated device ( $2.3 \mu\text{m}$ ) is much lower than the thickness desired ( $10 \mu\text{m}$ ) and the achieved cooling does not exceed  $2 \text{ K}$  in air and  $5 \text{ K}$  in vacuum, since all thermal energy is bypassed by the substrate (simulation results, using measured properties of the  $\text{Bi}_2\text{Te}_3$  and  $\text{Sb}_2\text{Te}_3$  films of the device). Thicker devices are under construction to achieve predicted performance.

## 5. Application

A self-calibrated pyrometer sensor is under construction. The pyrometer sensor is composed of a thermoelectric cooler and thermopile infrared detector—both based on the n- and p-type materials described above—and of an absorber, a black gold strip built on the membrane (Fig. 10).

The thermopile will be used to measure the temperature rise caused by radiation absorbed in the absorber. The Peltier cooler is used to stabilize the temperature of the cold junction of the thermopile at specific values. Finite element analysis, considering radiation and convection losses, shows the possibility to obtain a  $10 \text{ K}$  cooling of the sensor assuming a  $650 \mu\text{W mm}^{-2}$  thermal power absorbance in the absorber of the radiation sensor (radiation received on a  $300 \mu\text{m} \times 150 \mu\text{m}$  area at  $293 \text{ K}$ , emitted by a black body target object at  $373 \text{ K}$ , at a distance of  $1 \text{ m}$ ).

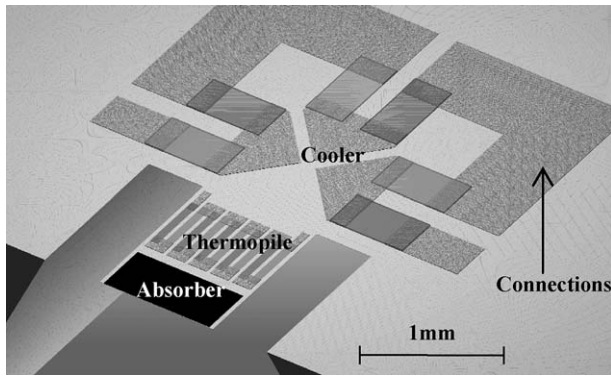


Fig. 10. The micro-pyrometer is composed of thermoelectric cooler, thermopile and a black gold strip.

The thermal power absorbed by the absorber of the radiation sensor is calculated with Eq. (5):

$$Q_{\text{RAD}} = \varepsilon\sigma(T_{\text{O}}^4 - T_{\text{S}}^4)A_{\text{S}} \quad (5)$$

$T_{\text{O}}$  and  $\varepsilon$  are the target object temperature and emissivity, respectively,  $T_{\text{S}}$  is the sensor temperature (controlled by the micro-cooler),  $A_{\text{S}}$  the absorber area and  $\sigma$  the Stefan–Boltzmann constant. The absorption factor of the absorber is omitted since is considered to be one.

In a pyrometer, the radiation absorbed depends on the difference between the (unknown) temperature and emissivity of the target object and the temperature and emissivity of the absorber. It is impossible to compute the temperature of the target object without correcting the reading with the emissivity of the target object. In order to realize the self-calibration method described elsewhere [11,12], several different temperatures of the sensor will be set by the Peltier device. The method (Fig. 11) uses different temperatures of the sensor ( $T_{\text{S1}}$  and  $T_{\text{S2}}$ ) to compute the emissivity and temperature of the target object [12]. The Peltier cooler has a small time constant because of its reduced dimensions, making it possible to set different temperatures of the sensor during the same temperature reading cycle, according to the patented self-calibration method [11]. The principle described is only valid when there is no object in the surroundings of the target object, which can reflect radiation into the sensor, using the target object as mirror surface. This effect is increased for high values of the target object reflectivity (which means low-emissivity, since the object is considered to have zero

$$U_1 = K \cdot \varepsilon \cdot \sigma (T^4 - T_{s1}^4) \quad U_2 = K \cdot \varepsilon \cdot \sigma (T^4 - T_{s2}^4)$$

$$T = \sqrt[4]{\frac{U_1 \cdot T_{s2}^4 - U_2 \cdot T_{s1}^4}{U_1 - U_2}}$$

$\varepsilon$ - Emissivity  $K, \sigma$ - constants

$T$ - Target temperature  $T_{sn}$  -  $n^{\text{th}}$  sensor temperature

Fig. 11. Principle used to compute the target temperature, using the values obtained by the micro-pyrometer cooled to different temperature [8].

transmittance). This error can be overcome by the use of more than two set points ( $T_{\text{S1}}$  and  $T_{\text{S2}}$ ) for the temperature of the sensor in order to compute the final target temperature independently of the surrounding reflections.

Industrial application of a network of micro-pyrometers for measuring the temperature of textiles in movement, operating in the 20–100 °C measuring range, representing a bandwidth of 5–20  $\mu\text{m}$  in wavelength, is the final goal of this work.

## 6. Conclusions

State-of-the-art  $\text{Bi}_2\text{Te}_3$  and  $\text{Sb}_2\text{Te}_3$  materials, with large figures of merit, were deposited by co-evaporation in the form of thin-films. The fabrication parameters (evaporation rates, substrate temperature and composition) were studied and optimized for best thermoelectric performance. Simulations of an in-plane (lateral) Peltier cooler made with these films, using electrical SPICE simulator or finite element analysis, show the possibility of achieving 10–20 K temperature differences between the hot and cold junctions. Results of simulations also reveal that the thickness and thermal conductivity of the supporting membrane affects significantly the performance of thermoelectric coolers. In order to demonstrate compatibility with flexible electronic concepts, a 25  $\mu\text{m}$ -thick polyimide foil was chosen as substrate due to its low-thermal conductivity and high upper working temperature. Future use of a standing bridge as a substrate, obtained by anisotropic etching of bulk silicon from the back of the wafer, covered by a layer of silicon nitride from the back of the wafer, will allow integration with silicon technology, but the higher thermal conductivity of the silicon nitride, when compared to Kapton<sup>®</sup>, will force the use of very thin bridges, in order to maintain the cooler performance. Future work will also focus on the use of an encapsulating silicon dioxide or silicon nitride layer deposited on the thermoelectric elements for protection and packaging.

## Acknowledgements

The authors would like to thank the Portuguese Foundation for Science and Technology (SFRH/BD/18142/2004) for funding this work and Gao Min from Cardiff University, for the guidelines on thermoelectric materials.

## References

- [1] G. Min, D.M. Rowe, Cooling performance of integrated thermoelectric micro-cooler, *Solid-State Electron.* 43 (1999) 923–929.
- [2] D.M. Rowe, *CRC Handbook of Thermoelectrics*, CRC Press, 1995.
- [3] R. Venkatasubramanian, E. Siivola, T. Colpitts, B. O'Quinn, Thin-film thermoelectric devices with high room temperature figures of merit, *Nature* 413 (2001) 597.
- [4] M. Ferhat, B. Liautard, G. Brun, J.C. Tedenac, M. Nouaoura, L. Lassabatere, Comparative studies between the growth characteristics of  $\text{Bi}_2\text{Te}_3$  thin-films deposited on  $\text{SiO}_2$ ,  $\text{Si}(100)$  and  $\text{Si}(111)$ , *J. Cryst. Growth* 167 (1996) 122–128.
- [5] H. Zou, D.M. Rowe, S.G.K. Williams, Peltier effect in a co-evaporated  $\text{Sb}_2\text{Te}_3(\text{p})$ - $\text{Bi}_2\text{Te}_3(\text{n})$  thin-film thermocouple, *Thin Solid Films* 408 (2002) 270.
- [6] H. Böttner, J. Nurnus, A. Gavrikov, G. Kühner, M. Jägler, C. Künzel, D. Eberhard, G. Plescher, A. Schubert, K.-H. Schlereth, New thermoelectric

- components using microsystem technologies, *J. Microelectromech. Syst.* 3 (2004) 414.
- [7] J.R. Lim, G.J. Snyder, C.K. Huang, J.A. Herman, M.A. Ryanand, J.P. Fleurial, Thermoelectric micro-device fabrication process and evaluation at the jet propulsion laboratory, in: 21st International Conference on Thermoelectronics, Long Beach, U.S.A., August 25–29, 2002, pp. 535–539.
- [8] A. Giani, A. Boulouz, F. Pascal-Delannoy, A. Foucaran, E. Charles, A. Boyer, Growth of  $\text{Bi}_2\text{Te}_3$  and  $\text{Sb}_2\text{Te}_3$  thin-films by MOCVD, *Mater. Sci. Eng. B* 64 (1999) 19–24.
- [9] A. Foucaran, A. Sackda, A. Giani, F. Pascal-Delannoy, A. Boyer, Flash evaporated layers of  $(\text{Bi}_2\text{Te}_3\text{--Bi}_2\text{Se}_3)_n$  and  $(\text{Bi}_2\text{Te}_3\text{--Sb}_2\text{Te}_3)_p$ , *Mater. Sci. Eng. B* 52 (1998) 154–161.
- [10] L.W. da Silva, M. Kaviany, Miniaturized thermoelectric cooler, in: ASME International Mechanical Engineering Congress and Exposition, New Orleans, U.S.A., November 17–22, 2002, pp. 1–15.
- [11] L. Hes, C. Couto, Method of contactless measuring the surface temperature and/or emissivity of objects, Patent 0 623 811 A1, (1994).
- [12] L.M. Goncalves, L.G. Gomes, S.F. Ribeiro, C. Couto, J.H. Correia, A miniaturized self-calibrated pyrometer microsystem, in: Proceedings of the 17th European Conference on Solid-State Transducers, Guimaraes, Portugal, September 2003, pp. 568–569.

## Biographies

**Luis M.V. Goncalves** graduated in 1993 and received his MSc degree in 1999, both in Industrial Electronics Engineering from the University of Minho, Guimaraes, Portugal. From 1993 to 2002 he researched on embedded systems, on Idite-Minho, an Institute to interface between University and Industry, Braga, Portugal. Since 2002, he has been a lecturer at the Department of Industrial Electronics, University of Minho, Portugal. He is currently working towards his PhD degree in Industrial Electronics and is involved in the research on thermoelectric materials for on-chip cooling and energy generation. His professional interests are thermoelectrics, microfabrication technology and microsystems.

**Carlos A.C.M. Couto** graduated in electrical engineering at University of Lourenco Marques, Mozambique in 1972. He obtained the MSc degree in 1979 and PhD degree in 1981 at UMIST (University of Manchester Institute of Science and Technology), UK, both in power electronics. In 1976, he joined the University of Minho in Portugal, where since 1995, he has been full Professor in the Department of Industrial Electronics. His research interests are microsystems, instrumentation and power electronics.

**Pedro Alpuim** received the PhD degree in Materials Science and Engineering from Instituto Superior Técnico, Lisbon, Portugal, in 2003. His PhD thesis was on the deposition and clean-room fabrication of amorphous and nanocrystalline silicon thin-film transistors and other devices on plastic substrates. Since 2003, he has been with the University of Minho in Guimaraes, Portugal, where he is an Assistant Professor in the Physics Department. There, he obtained support from European partners and from his own university to start a new lab on semiconductor thin-film deposition and characterization using CVD and PVD deposition techniques. His current research interests include thin-film devices for energy applications such as solar cells and thermopiles, flexible electronics and thin-film silicon-based optoelectronics for telecommunications.

**Michael Rowe** holds University of Wales BS degrees in both Pure Mathematics 1964 and Physics 1965 and a PhD 1968. In 1988, he was awarded a Doctor of Science for his contributions to the development of improved thermoelectric materials. He has held successive positions of United Kingdom Atomic Energy Research Fellow, Lecturer and Reader at the School of Engineering University of Cardiff, Wales and in 1994 was awarded a Personal chair in Electronic Engineering. Currently, Professor Rowe is Director of the NEDO Laboratory for Thermoelectric Engineering in the School of Engineering, Cardiff University and Deputy Head of the Electronics Division. He was a recipient of a British Gas Research Fellowship on two occasions 1977 and 1988—the only UK researcher to do so. In 1989, he received the outstanding technical paper award with Professor D.V. Morgan and Dr. J. Keily at the Eighth International Conference on Thermoelectric Energy Conversion, Nancy, France and in 1990 was runner-up for the British Electronics Week research activity of the year award. Professor Rowe has published more than 200 research papers and authored or co-authored three books on thermoelectrics and compiled and edited the CRC Handbook of thermoelectric—the first definitive text on this subject. In 1993, he was a European–Japanese visiting professor to the EEC laboratory Tsukuba and in 1994, a visiting professor to Centro Tecnico Aeroespacial, Brazil. Professor Rowe is a Fellow of the Institute of Physics—and off the Institution of Electrical Engineers. He is President of the International Thermoelectric Society and Deputy President of the European Thermoelectric Society.

**Jose Higinio Correia** graduated in Physical Engineering from University of Coimbra, Portugal in 1990. He obtained in 1999 a PhD degree at the Laboratory for Electronic Instrumentation, Delft University of Technology, working in the field of microsystems for optical spectral analysis. Presently, he is an Associate Professor in Department of Industrial Electronics, University of Minho, Portugal. His professional interests are in micromachining and microfabrication technology for mixed-mode systems; solid-state integrated sensors, microactuators and microsystems.